Testing automatic detection algorithms of volcanic unrest in SAR time series using synthetic data

Pierre Bouygues[1], Fabien Albino[1], Virginie Pinel[1]

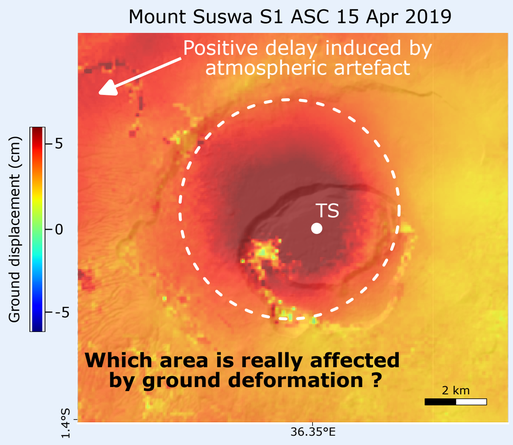
[1]Université Grenoble Alpes, Université Savoie Mont-Blanc, CNRS, IRD, Université Gustave Eiffel, ISTerre, Grenoble, France

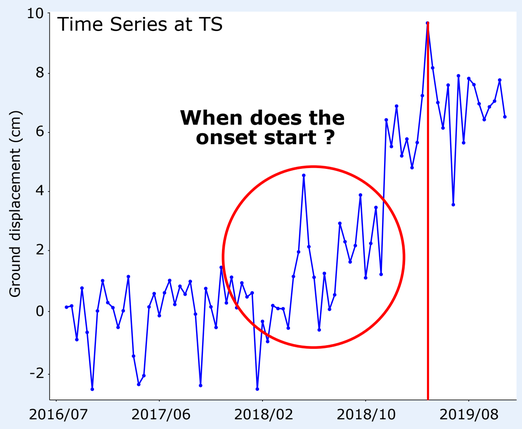
This presentation participates in OSPP
Outstanding Student & PhD candidate Presentation contest
Sharing not permitted

Introduction: Why is spatiotemporal detection important ?

Scientific Challenge:

Slow magmatic pressurization observed in **SAR time series** is often characterized by **low amplitude**, spatial variability and high level of noise (atmosphere, decorrelation, topography) leading to low signal-to-noise ratios (SNR) and making **early detection of the onset of deformation challenging**.

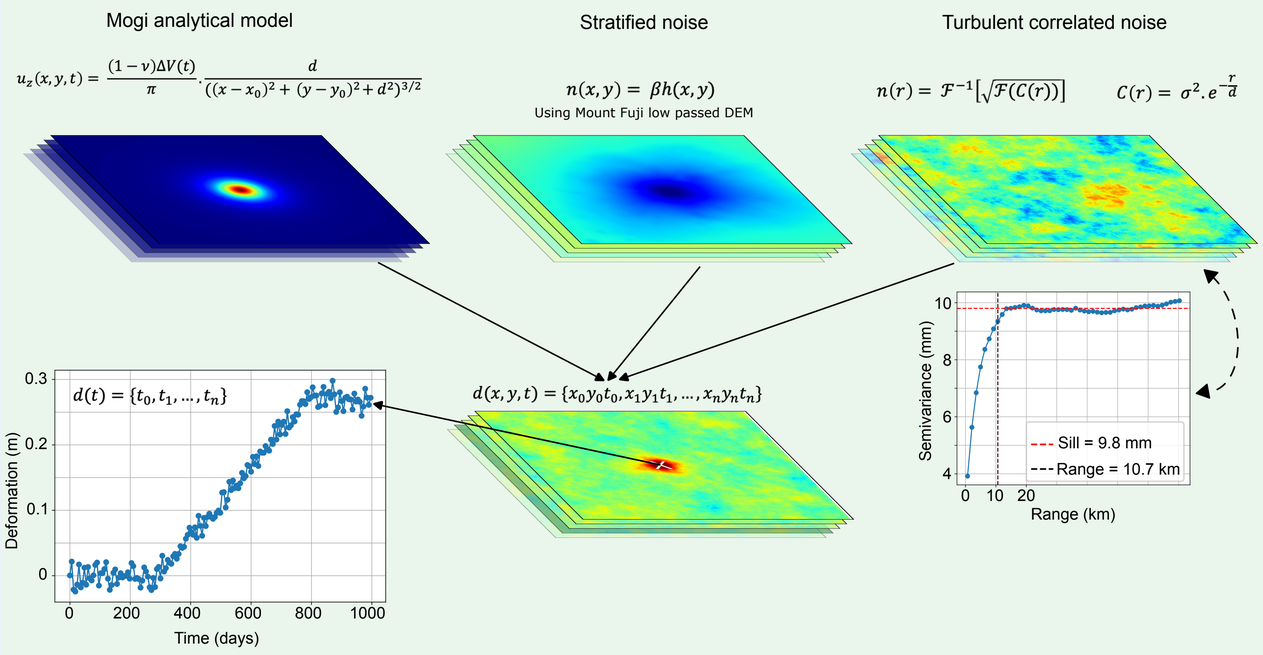




Objectives:

Testing the **reliability** of a **change point bayesian** framework do **detect** in **time** and **space** the **probabilty** of occurence of the **onset of the deformation** in **SAR time series**.

Method: Generation of synthetic displacement time series



Method: Bayesian Change Point Detection (BCPD)

With

Likelihood function

$$f(d_{i:j}) = \iint p(d_{i:j} \mid \beta, \sigma^2)\, p(\beta|\sigma^2)\, p(\sigma^2)\, d\beta\, d\sigma^2$$

probability to fit the data knowing the priors

from Ruggieri 2013

1.

Probability to have a CP at position τ in the window

$$P(\tau|d_{1:W}) \propto f(d_{1:\tau}) \cdot f(d_{\tau+1:W})$$

Before τ | After τ

adapted from Ruggieri 2013

Repeat for all windows and get the probability curve at one pixel of the cube

Displacement $d(t) = \{t_0, t_1, \dots, t_n\}$

Model: $d(t) = d \sim \mathcal{N}(X\beta, \sigma^2 I)$

Linear trend prior $\beta|\sigma^2 \sim \mathcal{N}(0, \sigma^2/k_0)$

Variance prior $\sigma^2 \sim Scaled - Inv - \chi^2(v_0, \sigma_0^2)$

from Ruggieri 2013

2.

Probability at time t to have a CP

$$P_{CP}(t) = \sum_{\tau=1}^{w} P(\tau|d_{1:W})$$

New step of the work

Method: Validation on synthetics

Binary classification criterias: $FP = False\ Positif$ $FN = False\ Negatif$ $TP = True\ Positif$ $TN = True\ Negatif$ With deformation is true for displacement > 2.5 cm

$$Recall = TPR = \frac{TP}{TP+FN}$$ *Are all events detected ?*

$$FPR = \frac{FP}{FP+TN}$$ *How many false alarms do we generate?*

$$Precision = \frac{TP}{TP+FP}$$ *Are detections correct ?*

$$Accuracy = \frac{TP+TN}{TP+TN+FP+FN}$$ *Are predictions correct ?*

$$F1 = \frac{2.TP}{2.TP+FP+FN}$$ *How well are detections balanced against false alarms?*

Mogi: (0, 0); depth = 8km

Deformation rate = 40 cm.y^{-1}

Start (d_{start}): day 300

Stop (d_{stop}): day 876

Time step (dt) = 6 days

Turbulent noise:
- Sill = 1cm & Range = 10km

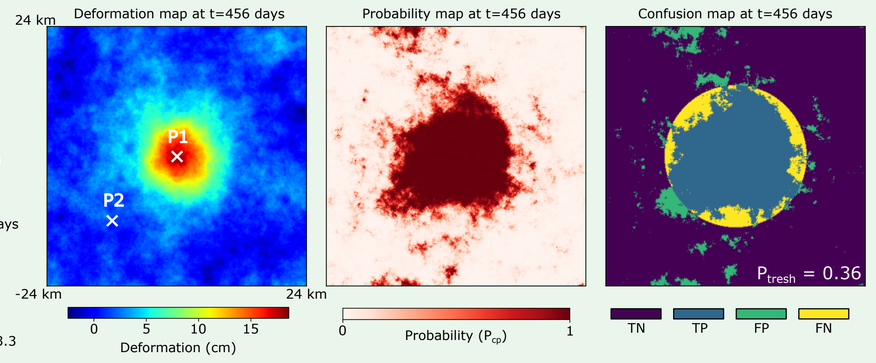
Stratified noise STD = 1cm

BCPD Window (W_i, W_e) = 288 days

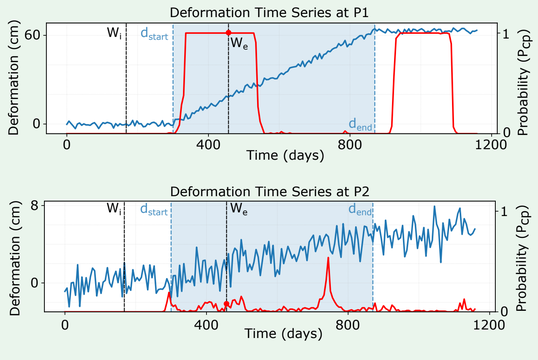
Priors: σ^2=1 cm / k_0 = 0.2

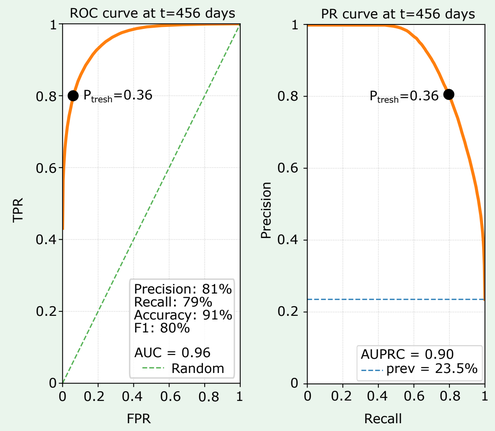
• P_{cp}(t=456 days)

First detection at t=336 days with a delay of 5dt and a SNR=3.3



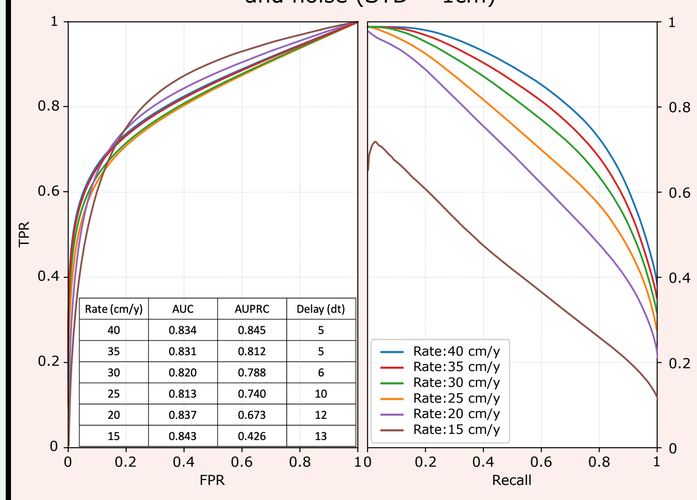
$$P_{tresh} = arg\max_{p} F1(P \geq p)$$





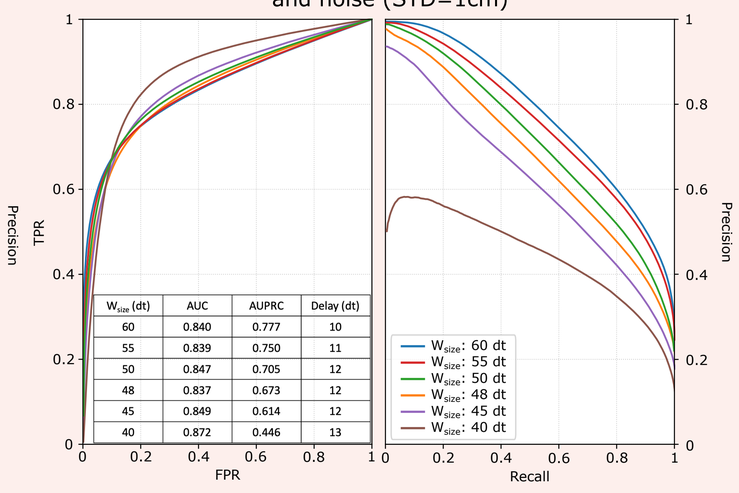
Results: Benchmarking on synthetic time series

Test 1: Decreasing rate with same window size (48 days) and noise (STD = 1cm)



Rate (cm/y)	AUC	AUPRC	Delay (dt)
40	0.834	0.845	5
35	0.831	0.812	5
30	0.820	0.788	6
25	0.813	0.740	10
20	0.837	0.673	12
15	0.843	0.426	13

Test 2: Decreasing window size (W_{size}) with same rate (20 cm/y) and noise (STD=1cm)

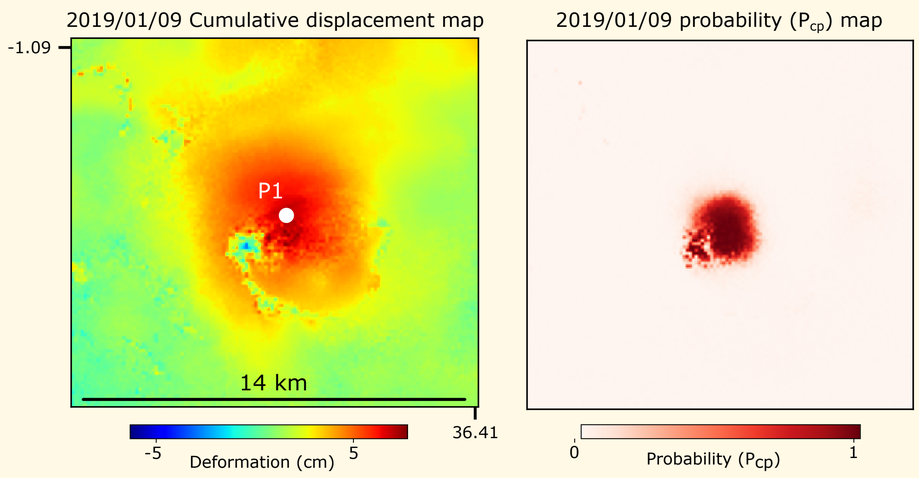


W_{size} (dt)	AUC	AUPRC	Delay (dt)
60	0.840	0.777	10
55	0.839	0.750	11
50	0.847	0.705	12
48	0.837	0.673	12
45	0.849	0.614	12
40	0.872	0.446	13

Results: Test on real SAR time series

Case study 1: Suswa Volcano - Sentinel-1 Ascending data (2016/07-2019/12)

Mount Suswa is the southernmost Holocene volcano of the Kenya Rift, a large (>700 km²) shield volcano with nested summit calderas, phonolitic–trachytic products, active fumaroles, and geothermal exploitation (Albino et al. 2021).



From Albino et al. 2021:

Radial deformation of 5km radius

Starting date: July 2018

Mean deformation rate: 4.3 ± 0.8 cm/yr

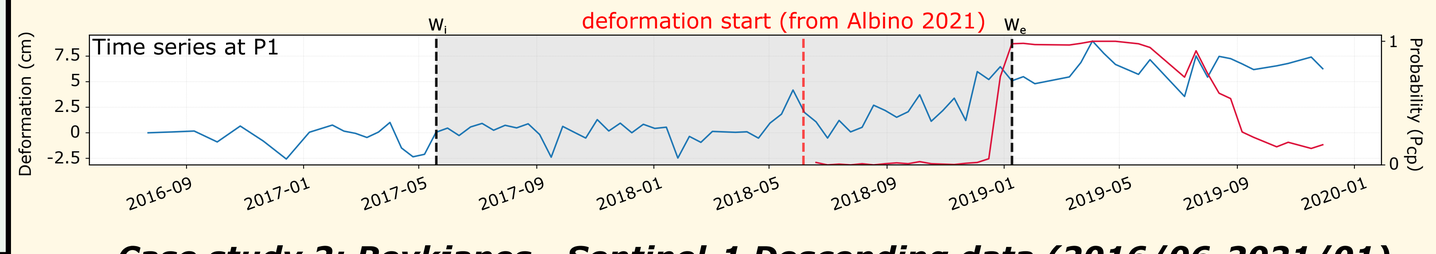
Run parameters:

Nb date = 87

Sigma = 2.5 cm

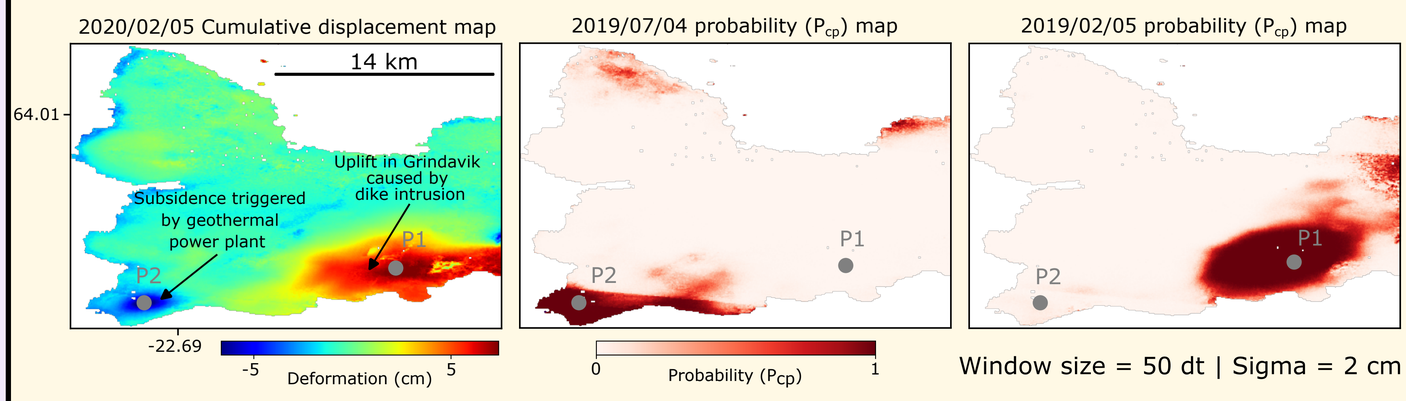
Window size = 50 dt

First detection the 9th january 2019

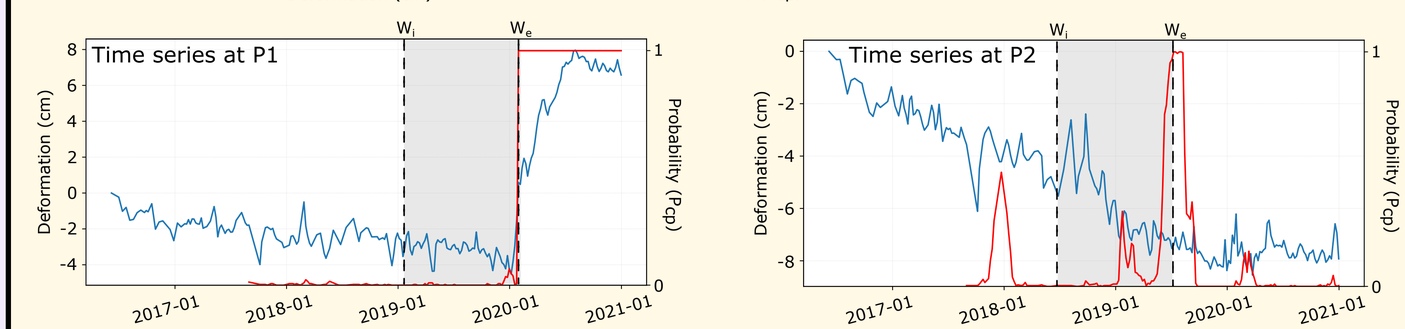


Case study 2: Reykjanes - Sentinel-1 Descending data (2016/06-2021/01)

The area exhibits two distinct deformation patterns: subsidence linked to geothermal extraction at Reykjanes to the west, and a shift from subsidence to uplift at Svartsengi in the east, interpreted as precursory to the 2021 Fagradalsfjall eruption (Biggs et al. 2022) . A total 219 cumulative displacement map were used from Sentinel-1 in descending orbit.



Window size = 50 dt | Sigma = 2 cm



Conclusion: Benefits and Limitations

What we learn from synthetic cases:

Metrics behavior:
* The **effectiveness** of the **method** is **evaluated** under **varying SNR conditions** (through changes in deformation rate) and different **temporal window sizes**.
* **ROC (AUC)** remains nearly **constant** when decreasing either the deformation rate or the window size, indicating **stable global binary discrimination**.
* **PR (AUPRC) decreases** significantly under the same conditions, reflecting a **loss in precision** for **detecting change points**.

As the **deformation rate decreases**, the **signal becomes less distinguishable from noise**, leading to more **false positives** and a **drop in precision**, while overall **ranking remains preserved**.
Reducing the **temporal window limits** the amount of information available to **constrain the model**, making **change points less well defined in time** and **increasing uncertainty**, which also **degrades precision** despite **stable ROC performance**.

What we learn from real cases:

With **slow deformation** and **noisy conditions** (Suswa), the **algorythm** was able to **detect** the **spatio temporal extent** of the **deformation** with the first probability on the 9 january 2019. The spatial extent of the CP allows to distinguish between areas affected by atmospheric noise and areas with **deformation.**

In rapid and **strong deformation** caused by dike **intrusion** in the case of Grindavik in early 2019, the **algorythm** was able to **detect without any delay**, the **spatio temporal extent** of the signal even if this signal was **preceded by a slow subsidence**.

Finally, the **algorythm** was also able to detect the **end** of a **long term subsidence** trend caused by the geothermal power plant in Reykjanes peninsula with a lot of **outliers** and **noisy** dates.

Bibliography

- Ruggieri, E. (2013). A Bayesian approach to detecting change points in climatic records. International Journal of Climatology,33(2), 520-528.
- Albino, F., & Biggs, J. (2021). Magmatic processes in the East African Rift system: insights from a 2015–2020 Sentinel-1 InSAR survey. Geochemistry, Geophysics, Geosystems, 22(3), e2020GC009488.
- Biggs, J., Anantrasirichai, N., Albino, F., Lazecky, M., & Maghsoudi, Y. (2022). Large-scale demonstration of machine learning for the detection of volcanic deformation in Sentinel-1 satellite imagery. Bulletin of Volcanology, 84(12), 100.